43rd AIAA/ASME/SAE/ASEE Joint Propulsion Conference & Exhibit
8 - 11 July 2007, Cincinnati, OH

AIAA 2007-5803

Lessons Learned In Solid Rocket Combustion Instability

Fred S. Blomshield[1]
Naval Air Warfare Center Weapons Division, China Lake, CA, 93555

Over the last 60 years, a considerable amount of time and money has been spent improving our understanding of combustion instability in solid rocket propulsion systems. Over this period, significant knowledge has been accumulated that can influence the acoustic stability of solid propulsive systems. Unfortunately, many of these lessons learned about combustion instability remain the knowledge of a select few in government and industry who work with combustion instability on a daily basis. This paper attempts to organize many of these "rules of thumb" that propellant formulators and motor designers need to be aware of in order to minimize the chances of combustion instability. In addition, several mathematical relationships are presented which can be used to predict the frequency of potential acoustic modes and determine resultant thrust oscillations produced by acoustic oscillations. Also included are some key fundamental equations which can be used to gain insight into combustion instability in rocket motor systems and there is a short section on motor instrumentation. This paper is not an attempt to be an exhaustive study into combustion instability, but rather, will attempt to list in a clear fashion some of the more important lessons learned and empirical observations of solid propellant combustion instability. This paper emphasizes composite propellants, but many observations apply to double base and composite modified double base propellants, as well.

Nomenclature

a	=	Speed of Sound	p	=	Pressure, also P
$A_{T,C,E}$	=	Nozzle, Chamber or Exit Areas	$\bar{P}$	=	Mean Pressure
AP	=	Ammonium Perchlorate	$\hat{P}$	=	Acoustic Pressure Amplitude, also $\hat{p}$
$\alpha_{\rho,\tau}$	=	Mode Coefficient	$\hat{P}_0$	=	Initial Acoustic Pressure Amplitude
α_X	=	Stability Alpha of Driving or Damping Term "X"	r	=	Burning Rate
c	=	Constant in Burning Rate Expression	R	=	Universal Gas Constant
ΔF	=	Thrust Oscillations	R_{pc}	=	Pressure-Coupled Response Function
ΔP	=	Pressure Oscillations	R_∞	=	Limiting Amplitude of Oscillations
f	=	Frequency (also F)	ρ	=	Density
F	=	Thrust	t	=	Time
L, R	=	Chamber or Passage Length, Chamber Radius	ρ	=	Radial Mode Number
L*	=	L-Star Characteristic Length	S	=	Surface Area
M	=	Molecular Weight or Mach Number	τ	=	Tangential Mode Number
n	=	Burning Rate Pressure Exponent or Node Number	u	=	Velocity (also v)
η	=	Thermal Diffusivity	$\hat{v}$	=	Acoustic Velocity
Ω	=	Non-Dimensional Frequency	V	=	Volume

I. Introduction

Solid propellant combustion instability is the amplification or attenuation of acoustic oscillations by solid propellant combustion processes in a rocket motor. Combustion instability in solid rocket propellant motors has been a continuing problem since the first rockets were used in World War II. Shortly after the war, research was begun trying to understand the phenomenon.[1,Price] Pressure oscillations can take the form of longitudinal, tangential

[1] Aerospace Engineer, PhD, Energetics Research Division, Code 474200D, 1900 N. Knox Rd, MS 6204, Senior Member AIAA
Approved for Public Release; Distribution is Unlimited.

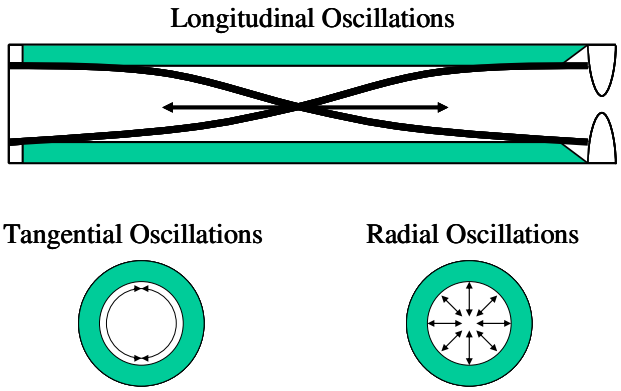

Figure 1. Solid Rocket Motor Acoustic Mode Types.

and, more rarely, radial oscillations. See Figure 1. The term linear instability refers to oscillations which are sinusoidal in nature and can be linearly decomposed into discrete sin waves. The term non-linear instability refers to oscillations which contain many acoustic modes and are often characterized by steep fronted non-sinusoidal waveforms. These oscillations cannot be linearized into discrete sin waves. This type of instability is often caused by injecta or debris passing through the nozzle which pulse the motor. Non-linear oscillations are often accompanied by DC pressure shifts and limiting amplitudes of the oscillations.

Often, combustion instability pressure oscillations are on the order of a few percent of the mean pressure and cause no problems with rocket motor performance. Occasionally, however, these oscillations can reach higher levels which can cause DC pressure shifts in the mean pressure, cause coupling effects with guidance and control sections, structural coupling, or, in the worst case, catastrophic motor failure. An example of a motor experiencing severe oscillations accompanied by large DC pressure shifts and subsequent motor failure is shown in Figure 2. Dozens of solid rocket motors developed over the last 60 years have experienced some form of combustion instability.[2,3] These motors experienced everything from minor linear acoustic oscillations to violent non-linear oscillations accompanied by large ballistic pressure shifts and in some cases motor destruction. In many of these systems considerable cost was added to the development or the programs were canceled. In others, after careful considerations of the consequences, it was decided to live with non-destructive oscillations.

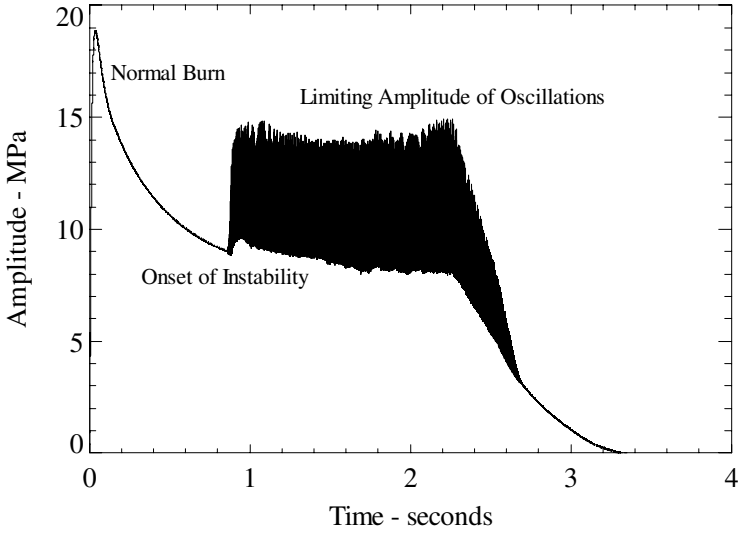

Figure 2. Example of Solid Motor Experiencing Severe Combustion Instability.

During development, solid rocket motors can experience different types and degrees of combustion instability. Due to these problems, considerable research has been performed during the last 60 years to investigate combustion instability.[4] Theories were developed in attempts to model primary physical mechanisms which influence combustion instability. These theories were at first purely one-dimensional in nature, but more recently have branched off into multi-dimensional and non-linear models of combustion instability. A brief overview of one-dimensional models will be presented in order to reinforce some of the empirical trends observed and provide the reader with some background. Empirical rules of thumb to prevent or at least minimize effects of combustion instability have been developed through experiences with many different solid motor systems. Some of these will be presented in this paper. Other techniques have also been developed over the years to predict at what frequencies instability might occur and what are the thrust oscillations induced by pressure oscillations. Many of these relationships will also be presented.

Hopefully, the content of this report will be of use to the propulsion community. An effort was made to reference many of the observations reported herein, however, many important references may have been inadvertently omitted which can reinforce (or add doubt) to the conclusions. I encourage all interested persons to report to me discrepancies, missing observations and missing references. Please send your comments or suggestions to Dr. Fred S. Blomshield, Code 474200D, M/S 6204, Naval Air Warfare Center, China Lake, CA 93555-6106, 760-939-3650, fred.blomshield@navy.mil.

II. Linear Stability Prediction

A. Driving Mechanisms

1) Pressure-Coupled Response: The pressure-coupled response is the amplification or coupling of the combustion processes taking place at the propellant surface with acoustic pressure. It is the often referred parameter to describe combustion instability characteristics of a propellant. The pressure-coupled response is mathematically defined as the ratio between the perturbed burning rate over the mean burning rate to the perturbed pressure over the mean chamber pressure:

$$R_{pc} = \frac{\hat{r}/\bar{r}}{\hat{p}/\bar{p}} \tag{1}$$

The non-dimensional R_{pc} is a function of burning rate, pressure, frequency and propellant physical and mechanical properties. Zero frequency corresponds to the steady state condition and the pressure-coupled response is the pressure exponent assuming the propellant burning rate obeys the classical St. Roberts burning rate law.[5]

$$r = c\bar{p}^{n} \tag{2}$$

Typical response curves taken by the T-burner are shown in Figure 3.[6] These curves all have classical shapes for composite propellants. This particular plot compares four similar propellants only differing by three percent of one ingredient. At zero frequency R_{pc} is the exponent and as frequency goes up so does the response to a maximum value of around 1.25 to 2.5 depending upon the propellant. As frequency gets even higher, the response falls off to zero. Double base propellants show a similar behavior except the fall-off to zero usually occurs at a much higher frequency. The T-burner is the most common way to measure response but numerous other devices can be used.[7,8] Other devices to measure the pressure-coupled response include the rotating valve, magnetic flow meter, microwave technique and the radiant heat flux device.[9,10,11,12,13]

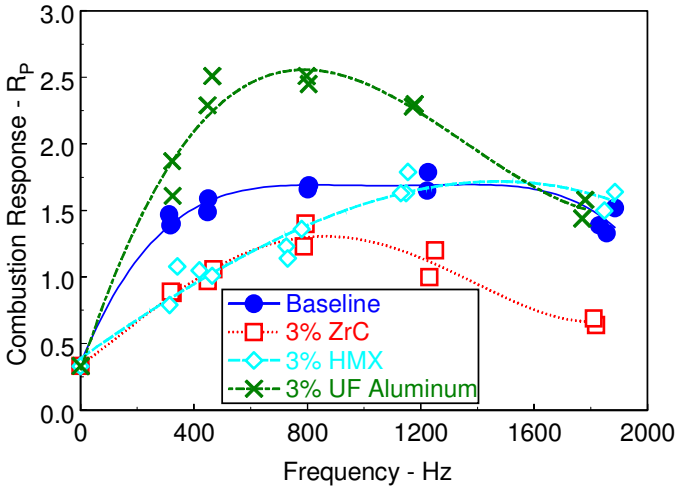

Figure 3 Typical Pressure-Coupled Response Curves

There are two main reasons for obtaining the pressure-coupled response of a propellant. First, it can be used to compare propellants destined for the same application. Once expected frequencies are known for a solid motor (this will be discussed later), the propellant with the lowest response will be less likely to drive instabilities, other factors remaining constant. It is very important to remember that combustion stability in a rocket motor is a system dependent phenomenon that depends on many factors such as pressure, geometry, structure, nozzle type, *etc*. The second reason for obtaining the response is that it can be used by motor stability prediction programs to compute the net driving by propellant combustion in a rocket motor.

2) Velocity-Coupled Response: The velocity-coupled response is the amplification or attenuation of combustion processes taking place at the propellant surface by the acoustic velocity.[14] Unlike the pressure-coupled response which has broad support for its basic definition and nature, the velocity-coupled response definition does not share this universal support. Many experts do agree that velocity coupling does correspond to the non-steady component of erosive burning. Recent research indicates that velocity coupling is a non-linear phenomenon and that conventional linear approaches cannot be applied.[4,15,16,17] Unlike acoustic pressure, acoustic velocity varies in both the longitudinal direction and in the radial direction due to a thick acoustic boundary layer. Because of these variations, the acoustic velocity can have phase differences in both radial and longitudinal directions. How the specific mechanisms of velocity coupling can be applied to motor stability is beyond the scope of this report. Fortunately, velocity-coupled response driving is believed to be very small for many motors. However, some combustion instability problems, particularly non-linear problems, indicate velocity coupling can be an important driver of combustion instability.

3. Distributed Combustion: The third driving mechanism is called distributed combustion response. Distributed combustion response is the interaction of the acoustic field with burning metal particles taking place away from the propellant surface. This phenomenon is only a factor when dealing with highly metallized propellants, and only occurs in those whose burning characteristics allow the metal to burn in a distributed manner throughout a motor chamber. There have been several research efforts examining this phenomenon.[18,19] Because it occurs in a relatively small percentage of motors, it will not be discussed in any great detail in this paper.

B. Damping Mechanisms

1. Nozzle Damping: The principle damping mechanisms in a solid motor are nozzle damping, particle damping, mean flow/acoustic interactions and structural damping. Nozzle damping is usually the largest damping mechanism in a motor, particularly with longitudinal and mixed transverse/longitudinal modes. Conceptually, it is simple. As acoustic pressure waves come in contact with the nozzle throat of a motor, some of this energy is transmitted through the throat and radiated out to the environment. The theoretical prediction of nozzle damping is very well established.[20,21,22,23]

2. Particle Damping: Particle damping only applies to propellants containing solid species in the combustion products, such as metallized propellants or those with acoustic stability additives. The amount of particle damping is dependent on the mass fraction of particles in the flow field and, most importantly, particle size. Larger particles damp lower frequencies, while smaller particles damp out higher frequencies. The calculation of particle damping is also well established.[6,20,24,25] Figure 4 shows relative particle damping versus particle size for six different frequencies. This plot was computed using mono-sized particles of the same mass fraction.[6,26,27] It is important to note how higher frequencies are much more efficiently damped than lower frequencies for the same mass fraction of particles. Figure 5 is a useful curve that indicates optimum particle size to damp a particular frequency. Both Figure 4 and Figure 5 are for typical solid propellants and are reasonably insensitive to formulation.

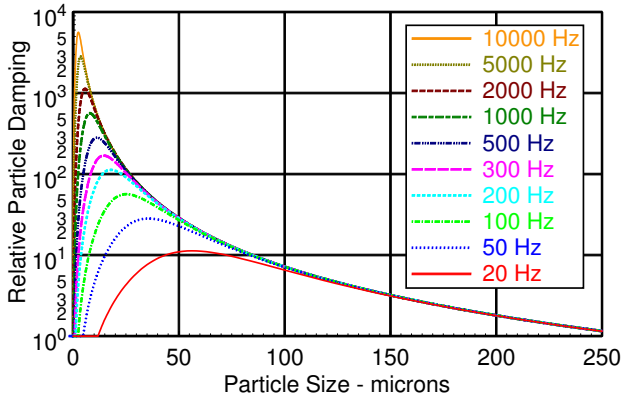

Figure 4 Relative Particle Damping versus Particle Size at Six Frequencies.

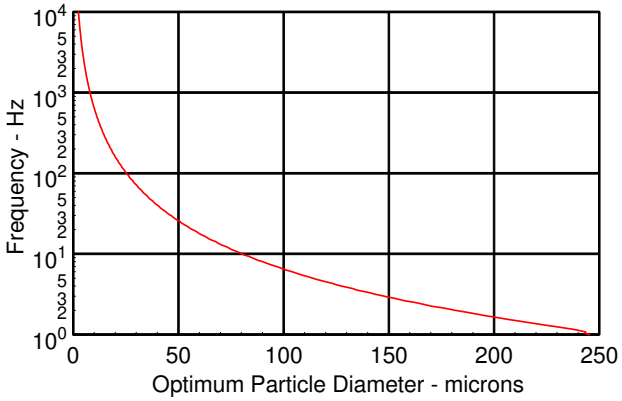

Figure 5 Optimum Damping Particle Size versus Frequency.

3. Flow Interactions: Mean/acoustic flow losses are those losses associated with mean flow interactions with the acoustic field. There are generally two schools of thought as to how this occurs for flow near the surface of the propellant in the boundary layer. The first is called flow turning losses.[28,29] Conceptually, this is the work done to incoming flow as it acquires acoustical motion.[20,21,23] Combustion products enter normal to the surface and must be accelerated to the axial direction. That change of direction is the origin of the term "flow turning."[4] The second method to examine the acoustic boundary with flow normal to the surface is called boundary layer losses.[30,31,32,33] It is sometimes known as the "Flandro boundary layer term." Understanding the phenomenon often deals with vorticity and acoustic boundary layers. Another type of flow interaction which is separate from the above terms is vortex generation of flow around sharp corners.[34,35,36,37] Large segmented boosters can have this type of acoustic coupling.[38,39] The final type of flow interaction is referred to as wall losses. These are frictional losses resulting from flow over exposed case walls. Often this term is small, since usually there is little exposed case walls.

4. Structural Damping: The final damping mechanism is structural damping. As the name implies, this is damping due to deformation of the motor structure due to acoustic pressure oscillations. The motor structure can include the actual case as well as the motor liner. Normally, this is thought to be very small compared to other losses in all but

very large rocket motors where acoustic loading can be great. Elastic exposed case liners can also make this term significant. A pictorial representation of all of the gains and losses in a solid rocket is shown in Figure 6.

C. Motor Stability

Linear stability theory has been successfully applied to the prediction of solid propellant rocket motors.[40,41,42,43,44,45,46] The linear assumption implies that the change of acoustic pressure amplitude in a motor can be expressed as an exponential. The following equation can be used:

$$\hat{P} = \hat{P}_0 \, e^{\alpha_M t} \tag{3}$$

Here, $\hat{P}$ is the acoustic wave amplitude, $\hat{P}_0$ is the initial amplitude value, α_M is rate of acoustic energy change in the motor and t is time. If α_M is negative, the motor is stable, if α_M is positive, the motor is unstable. The stability of a solid rocket motor is determined by the net sum of acoustic gains and losses in the system. The linear assumption further assumes that the contributions to motor stability can be simply added and subtracted to determine a motor's total stability, α_M. The linear relationship for total motor alpha is:

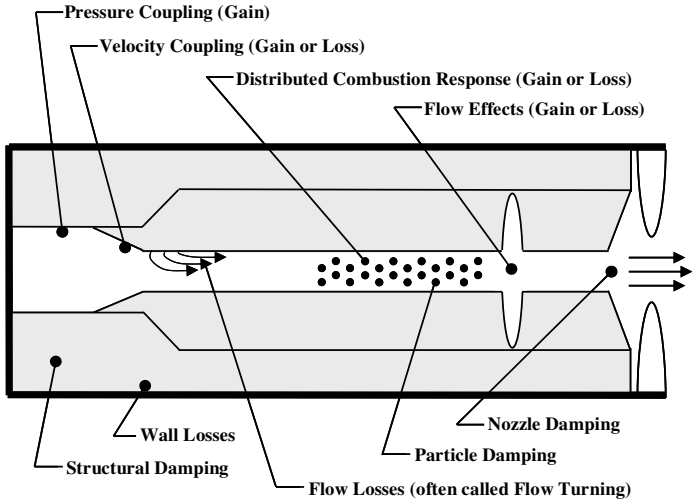

Figure 6. Acoustic Energy Gains and Losses in a Solid Rocket Motor.

$$\alpha_M = \alpha_{PC} + \alpha_{VC} + \alpha_{DC} + \alpha_{NOZ} + \alpha_{PART} + \alpha_{MF} + \alpha_{SD} \tag{4}$$

In Eq. (4), α_{PC}, α_{VC} and α_{DC} is the driving terms due to pressure coupling, velocity coupling and distributed combustion, respectively; and α_{NOZ}, α_{PART}, α_{MF} and α_{SD} are the damping terms due to nozzle damping, particle damping, mean flow interactions and structural damping, respectively.

Sample stability versus time plots for a reduced smoke solid rocket motor are shown in Figure 7 and Figure 8. Figure 7 shows the total motor stability alpha, α_M, at three different motor pressures for the same motor geometry and propellant. Figure 8 shows the driving, damping and total stability alphas for a single motor. These curves were calculated using the Standard Performance Prediction/Standard Stability Program (SPP/SSP) code developed under both Air Force and Navy sponsorship and recently improved to predict non-linear motor behavior.[47,48,49,50,51] The inputs to this program include complete motor geometry and detailed propellant properties, including the propellant response function. The program uses a grain design and ballistic code to provide inputs to the stability module. The program allows prediction of linear motor stability as a function of time with a single set of inputs.

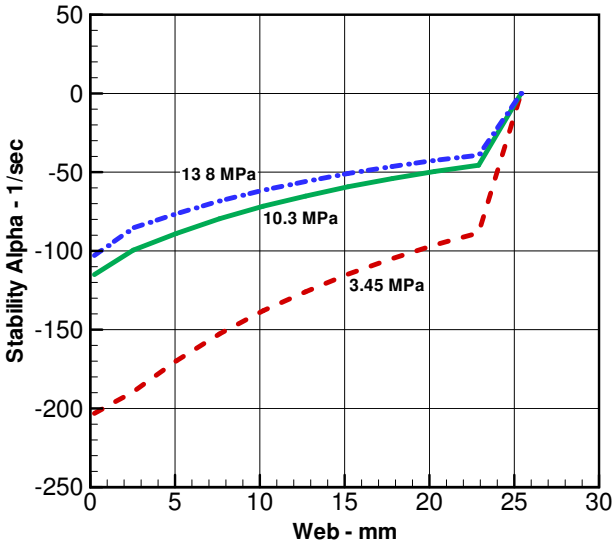

Figure 7. Total Motor Stability at Three Pressures.

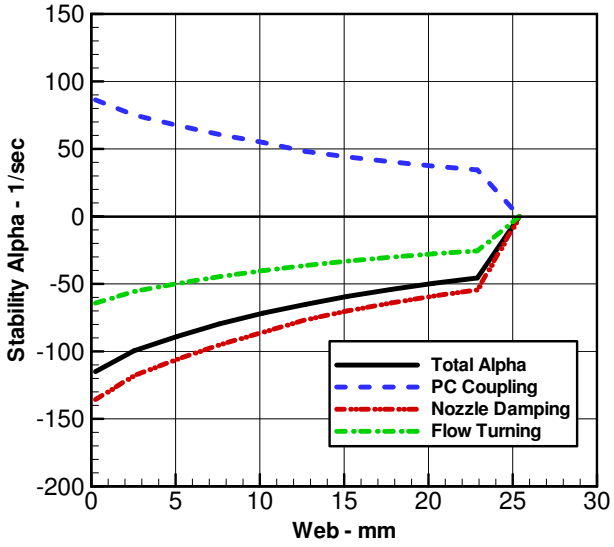

Figure 8. Detailed Motor Stability Map.

D. Stability Observations

The following section describes some theoretical observations or trends for solid propellants and solid rocket motor combustion instability which have a theoretical background. Many of the following statements have experimental evidence to reinforce the theory.

Looking at total motor stability in Figure 7 and Figure 8, the difference between the value of motor stability and zero damping is often referred to as the limit or margin of linear stability. For many motors the magnitude of this margin becomes smaller as the motor burns. This implies that the tendency of a motor to become unstable often increases with time.[36,40,41,45,46,47,52] Referring to Figure 8, it can be seen that the magnitude of both driving alphas (those that are positive) and damping alphas (those that are negative) decrease in magnitude as the motor burns to completion. This can be explained by examining the following expression:

$$\alpha_X = \frac{\oint_{Burning\ Surfaces}(...)dS}{\oint_{Internal\ Volume}(...)dV} \quad \begin{matrix}\text{(Usually Constant)} \\ \\ \text{(Always Increases During Burn)}\end{matrix} \tag{5}$$

Except for particle damping, all driving and damping alphas can be written in this form. The subscript "X" refers to various terms. The burning surface area of most motors is reasonably constant, while the internal volume is always increasing as propellant is consumed. This implies that as the motor burns, the magnitude of the various alphas, $|\alpha_X|$, will become smaller. For metallized systems where particle damping is significant, total motor stability approaches the particle damping alpha as the motor burns to completion. This is because the level of particle damping for typical motors is constant due to a constant burning surface area. As a general rule, if a reduced smoke propellant rocket is to be unstable, it will be toward the end of burn. If a metallized propellant rocket motor is to be unstable, it will be earlier in burn compared to a non-metallized system. Figure 9 depicts this graphically.

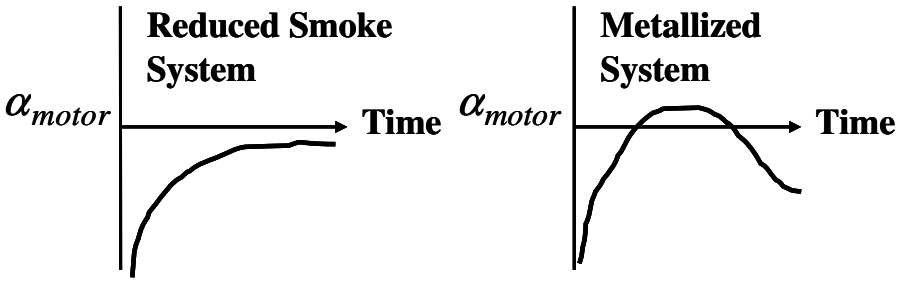

Figure 9. Total Motor Stability Alpha versus Time for Systems with and without Particle Damping.

As a general rule of thumb, motor designer should not design a motor with the majority of burning area in aft end.[40,41,45,46,52,53] A star aft geometry is an example. The driving mechanisms of velocity coupling and distributed combustion have terms like the following:

$$\oint_{Burning\ Surface} \hat{p}\hat{v}\overline{u}(...)ds \tag{6}$$

At the aft end of the motor, both mean velocity, $\overline{u}$, and oscillating pressure, $\hat{p}$, become large. ($\hat{v}$ is the oscillating velocity.) Because of these terms, the magnitude of velocity coupling and distributed combustion terms can be large in magnitude. This will tend to make a motor less stable. Nearly all stability integrals have a $\hat{p}$ in them. For longitudinal oscillations, $\hat{p}$ is very close to zero near the center of the motor from front to back. Ideally, most of the surface area should be at the center of the motor with little burning surface at the ends to minimize driving stability integrals. Unfortunately, this makes it very difficult to remove the casting mandrel using conventional motor casting techniques. For these reasons, the forward end is the recommended location for most of the burning surface area.

Raising the mean operating pressure in a motor will tend to make the motor less stable. Raising the mean pressure decreases both nozzle damping and flow turning losses. This can lead to lower margins of stability and small changes in the propellant response can lead to an unstable motor. Figure 7 shows the effect on total motor stability as chamber pressure is increased.

III. Empirical Observations

The following observations are primarily empirical in nature, but often have some theoretical basis as well. Although they are grouped by category, it is important to remember that some items could be listed under multiple categories.

A. Burning Rate, Pressure and AP Particle Size

Various observations about burning rate, pressure and ammonium perchlorate (AP) particle size can be made as to their effects on combustion instability. These effects are grouped together, as they are often interrelated.

1. Very fine and ultra fine (less than 1 micron) AP oxidizer particles usually give high pressure-coupled response within a given propellant burning rate group.[54,55] Propellants with fine AP have been known to cause significant combustion instability behavior in motors. Particles less than 5 microns in diameter should be used with caution.

2. In general, if AP particle size is constant, a higher burning rate will give a lower pressure-coupled response.[54] This appears to be at odds with (1) above. If AP particle size is held constant, higher burning rates can be obtained by the use of different binders, with additives and/or with catalysts.

3. Very coarse AP, i.e., greater than 200 microns, can and lead to motor instability problems. In addition, there is some evidence the coarse AP causes an increase in the non-linear acoustic erosivity.[56,57]

4. The propellant response function shows a strong dependence on mean pressure, although the pressure at which the propellant response function is a maximum changes among different propellant types and burning rates.[54] The response function dependence on pressure is well known, but at what pressure the response is a maximum at a particular frequency can only be determined by some form of response testing. The most common form of testing is the T-burner.

5. Propellants with a low pressure exponent, n in Eq. (2), will, in general, have a lower response function. Propellants with zero or negative pressure exponents such as mesa burning propellants, are very desirable from a combustion instability point of view.[58] The lower the pressure exponent, the better.

6. In general, as mean motor pressure is increased, other factors remaining the same, a motor will tend to become less stable.[40,41,45,46,52,55,59] Raising mean motor pressure reduces the margin of stability due to decreases in both nozzle and flow turning losses, see Figure 7. Furthermore, a stable motor will tend to be more susceptible to non-linear pulsed instability.[40,45,46,52,59,60,61] An example of this is shown in Figure 10. This plot presents the ballistic pressure traces for three identical motors except for nozzle throat sizes which modify the motor chamber pressure.[42,45,46] These motors were all pulsed. The lowest pressure motor could not be pulsed into instability. The middle pressure motor was pulsed late in burn and non-linear longitudinal instability was triggered with DC pressure shifts. The highest pressure motor experienced violent spontaneous tangential mode instability that caused extreme chamber pressure increases and eventually motor failure. All three motors had the same geometry and propellant.

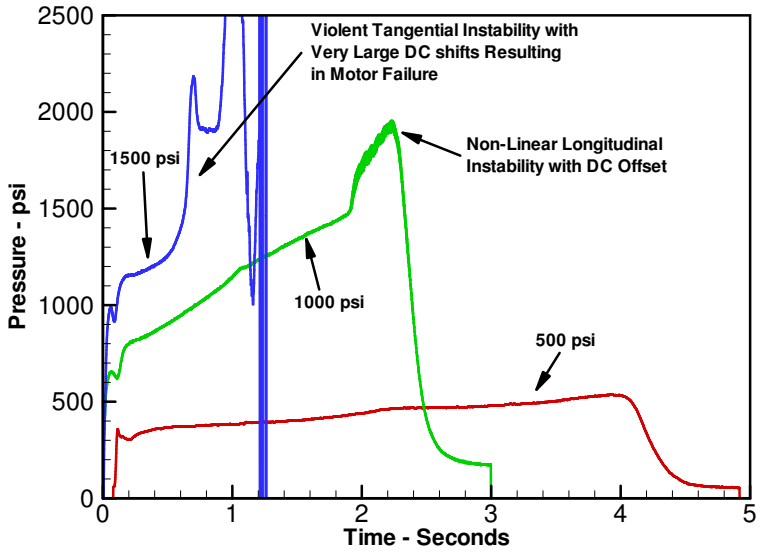

Figure 10. Example of Motor Pressure Effect on Combustion Instability.

To summarize these statements, if one increases burning rate with catalysts, propellant combustion response will tend to go down. If one increases burning rate with fine AP, propellant combustion response will tend to go up. Very fine or very coarse AP is not good from a combustion instability point of view. These effects can be explained by the following; for very fine AP crystals burning in a fuel binder, chemical reaction processes are kinetically controlled and have a relatively high reaction order. The reaction order is the pressure exponent in the chemical reaction equilibrium equation. For very large AP crystals, combustion is controlled by an AP mono-propellant flame which also has a high reaction order. In between the extremes of particle size, combustion processes are believed to be controlled by more diffusional effects which are not as sensitive to pressure oscillations.[62]

B. Flow Effects

Flow effects due to internal geometry of a solid rocket motor can contribute to the stability of a motor. The following observations help illustrate this point.

1. The design of a motor should minimize flow around sharp edges. These can lead to vortex shedding, which can couple with internal motor acoustics.[34,35,36] Avoid protruding grain inhibition or actual propellant geometries in which the flow is constricted in the longitudinal direction and avoid radial slots like those used for stress relief.

2. Oscillations created by vortex shedding are usually small in amplitude, i.e., less than 1 percent. Vortex shedding is a more common problem in large segmented boosters like the space shuttle solid rocket motors. In these motors, internal motor flow around sharp corners between segments leads to vortex shedding. Oscillations in the SRM and RSRM are believed to be caused by coupling between these large scale vortices and acoustic modes of the motor chamber.[63,64] Because of their size, these frequencies are typically very low, less than 50 Hz. As mentioned above, these oscillations are low in magnitude, however, it must be remembered that a single psi of pressure oscillation can lead to hundreds of thousands of pounds of thrust oscillations in large motors. How to determine these thrust oscillations will be discussed later

3. The grain design should not have an abundance of burning area in the aft end.[40,41,45,46,52,53] This can increase driving due to velocity coupling and distributed combustion for metallized propellants. This can also decrease nozzle damping if more of the aft case is exposed as the motor burns.

4. Multiple nozzles should be more stable due to increased nozzle damping. However, the design must be done correctly. A large flat aft end surface among the nozzles can reflect acoustic waves very efficiently.[56] The area between the nozzles must be designed as to not reflect acoustic waves. The nozzle entrance angle is also an important parameter. There is experimental evidence that a submerged nozzle with reverse cavity flow slightly reduces the effective nozzle damping.[65] Because nozzle damping is one of the principle damping mechanisms, small changes in aft geometry and nozzle type and placement can lead to big changes in motor stability.

5. For star, wagon wheel, or other similarly slotted geometries, the number of star points should be an odd number. An odd number of slots will reduce tangential mode oscillations due to the geometry and internal flow to. A four point star, for instance, might encourage a second tangential mode. However, recent evidence suggests that this may not necessarily be true and that the number of slots makes no difference.[66]

6. L* (L-Star) is a type of non-acoustic instability which often occurs near the beginning of motor burn immediately after ignition when the chamber volume is small and the chamber pressure is low. As its name implies, this form of non-acoustic combustion instability does not correspond to an acoustic mode of a rocket motor. Non-acoustic combustion instability results from a coupling between the combustion and the blow-down or characteristic time of the rocket chamber. Thus, in an acoustic wave, the pressure varies both in time and space, through the chamber, according to an acoustic mode. In contrast, during a manifestation of non-acoustic combustion instability, the pressure is constant throughout the chamber, varying only in time. The sensitivity to L* instability (sometimes called chuffing or sputtering) is related to motor volume over the nozzle cross sectional area, $L^* = V/A_T$.[67] The lower the L*, the more likely a motor will experience L* instability. Figure 11 is a compilation of many L* values for a variety of propellants and indicates both stable and unstable combustion regions.[57] This figure is a general guide to when a propellant in a motor might be unstable.

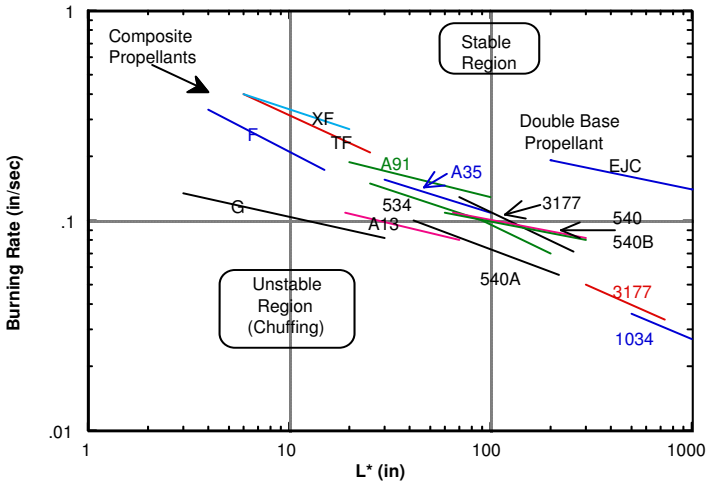

Figure 11. Non-Acoustic Combustion Instability Boundary for a Variety of Solid Propellants.

C. Particle Effects

Particles in the combustion products, both inert and burning, can have a significant effect on combustion instability. The effect of particles on acoustics has been studied for many years, and its specific application to solid rockets has evolved over the past forty years. Inert particles include aluminum oxide, Al_2O_3, produced from aluminum combustion and stability additives such as zirconium carbide, ZrC, or inert Al_2O_3 added to the propellant during mixing. These particles cause the particle damping mentioned above. Stability additives are crucial ingredients in nearly every modern reduced smoke, composite propellant formulation in use today. They have been proven very effective in reducing and/or eliminating combustion instability in many solid rocket systems. In one recent study numerous reduced smoke composite propellant tactical sized rocket motors were intentionally pulsed.[6,40,52] Many of the motors containing propellants without additives were pulsed into violent unstable non-linear instability, accompanied by extensive DC pressure shifts, and often resulted in nozzle or motor case failure. These same motors, cast with propellants containing one percent ZrC, 8µm Al_2O_3 or 90µm Al_2O_3 in place of one percent the ammonium perchlorate (AP), could not be pulsed into unstable behavior even when pulsed twice as hard. Figure 12 shows this amazing effect graphically. Burning metal particles can cause a distributed combustion coupling with internal motor acoustics and drive instabilities. For most metallized propellants, metal particles burn very close to the propellant surface and do not have time to couple with the acoustics. However, evidence suggests that these burning metal particles can contribute to combustion instability for high burning rate propellants at high pressure through the mechanism of distributed combustion. Below are some observations about combustion instability behavior of particles in solid rocket motors.

1. Particle damping at a particular frequency is very dependent on particle size (see Figure 5). [6,26,27]

2. Given equal mass fractions of particles, smaller particles are much more efficient at damping higher frequencies than larger particles are at damping lower frequencies (see Figure 4). [6,26,27]

3. Some additives are effective in reducing combustion instability behavior of solid propellants. This is done by the reduction of the propellant response function and by increasing particle damping. [6,40,40,52,53,60]

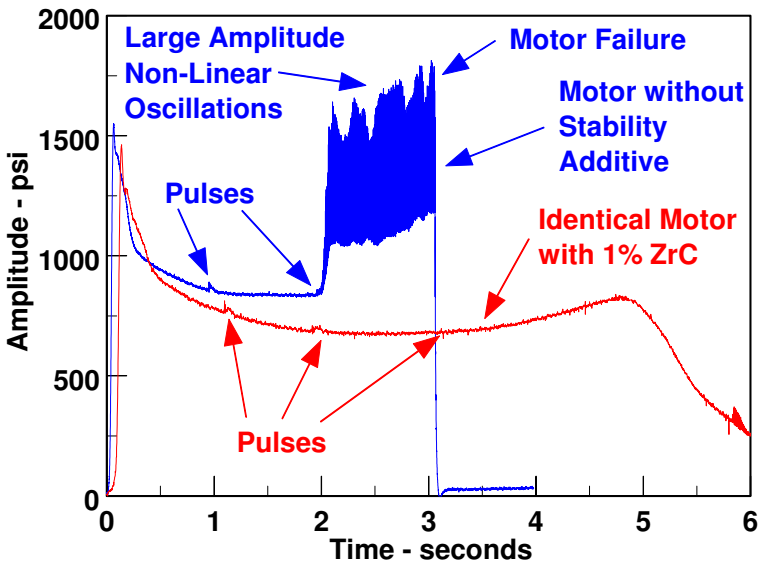

Figure 12. Motor Stability with and without Stability Additive.

4. Particulates in the flow are very non-linear in nature.[40,52,60,68] This means that linear theory does not predict the observed behavior of particles in solid rocket motors. The very nature of particle damping causes one particle to damp out many different acoustic modes, adding to the non linearities.

5. The effect of distributed combustion on high burning rate, metallized propellants at high pressure may not solely be due to an increase in acoustic driving by burning aluminum particles, but also a lowering of particulate damping

at the desired frequency due to a reduction in the normally damping Al_2O_3 particles. These burning particles are damping as well, but at different frequencies. The net distributed combustion result is less particle damping at the desired frequency of oscillation.[18]

6. For high burning rate propellants at high pressure, there is a direct relationship between aluminum particle size and combustion response. The smaller the aluminum particle size, the higher the response.[18] For conventional burning rate propellants at lower pressure, there is some evidence that smaller aluminum particles may yield a lower response.[55,56] There is also evidence that the type of aluminum, i.e., flake or particulate, as well as aluminum coatings, such as grease, can effect the combustion response of propellants.[55,56] To be certain, aluminum particle size and type effects on combustion response must be measured for different classes of propellants.

7. Metallized propellants produce a bimodal or trimodal distribution of Al_2O_3 particles that will be present in the combustion chamber.[18] The smaller size fraction is often around 1 micron and is directly produced by the burning aluminum particles in the propellant. The larger size fraction is produced by metal agglomerations at the surface and is often as large as 200 microns. The acoustic damping is strongly dependent upon the particle size, see Figure 4 and Figure 5. The relative mass fraction of the fine and coarse size fractions is usually determined experimentally by burning a propellant sample in a particle collector. After careful size analysis the particle damping can be computed.

D. Chemistry Effects

This area is very important in determining combustion instability behavior of propellants. Unfortunately, it is also the area that lacks good experimental evidence to understand the controlling mechanisms that cause some propellants to respond to pressure oscillations and some not to respond to pressure oscillations. The following observations are based mainly on theoretical predictive modeling and are somewhat speculative.

1. A propellant with an energetic pressure dependent diffusion flame is more likely to have instability problems. AP propellants typically have this form of flame. CL-20 and ADN oxidizer propellants have this type of flame to a lesser extent. HMX oxidizer propellants do not have this type of flame and would typically drive less instabilities than AP based propellants.[69]

2. Preliminary results indicate that CL-20 and ADN will have very weak diffusion flame with inert binders. This will result in very small particle size effects on burning rate (like HMX).[70] This probably indicates that CL-20 and HMX particle size variations will have little impact in combustion instability behavior.[69]

3. Initial evidence shows that ADN has a low melting point, low surface temperature and low pressure exponent which tends to indicate a significant condense phase reaction on the surface. In general, the greater the condensed phase reactions, the higher the temperature sensitivity which, in turn, could lead to instability behavior.[57]

4. The higher the temperature sensitivity, the more likely a propellant will be subject to combustion instability.[1,Kubota] Of the observations in this section, this one has the most substantiated experimental and theoretical basis.

E. Non-Linear Effects

The area of non-linear instability is an area in which recent progress has been made. There have been numerous papers on the subject covering both experimental observations and modeling.[4,30,31,32,33,40,41,45,46,49,50,51,52,53,59,60,61,66,68,71,72,73] The details of this work is well beyond the scope of this report. Some important conclusions and comments about non-linear combustion instability can be made. Non-linear behavior is a function of hardware (motor or test) with dependence on burning rate and response function values over all frequencies. The term non-linear implies many different harmonic modes are all excited simultaneously and the system cannot be linearized into discrete wave forms. This type of instability is often caused by injecta or debris passing through the nozzle which pulse the motor. Non-linear oscillations are often accompanied by DC pressure shifts and oscillation limiting amplitudes.

1. Non-linear stability is dependent upon propellant response over the entire frequency range.[4,15,40,45,46,52,68] Non-linear combustion instability is believed to be related to energy feedback from higher harmonics to lower harmonics.

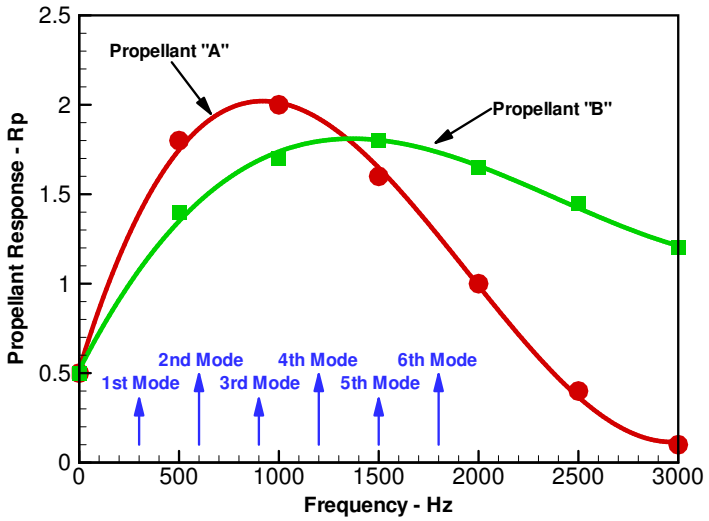

Figure 13. Illustration of Response Function effect on Non-Linear Stability.

In Figure 13 propellant "A" has a higher response peak while propellant "B" has a much broader response peak that stays high as frequency increases. Propellant "A" should be more stable from a non-linear point of view since propellant "B" will be more susceptible to amplifying non-linear high frequency waves.

2. Pulsing a motor can give quantitative information to determine how stable that motor is. Pulsing can be used to determine the margin of stability. If this knowledge is known, motor developers can feel much more confident about changing, for example, AP particle size or manufacturer without causing the motor to become unstable.[40,45,46,52] Good examples of motor pulsing are shown in Figure 2 and Figure 12.

3. Stability additives can be very effective in eliminating pulsed non-linear instability.[6,40,52,60,68] Figure 12 is an example of this. The additives work by reducing the combustion response over a broad frequency range and by increasing the particle damping. Figure 13, although only an illustration, shows how a stability additive might reduce the response at higher frequencies. In this example propellant "A" would have the stability additive. The pulse amplitude required to trigger non-linear instability will be increased and the DC shift and instability wave amplitude decreased with the addition of stability additives.[40,45,46,52,60,61]

4. One parameter that has been used to rank propellants in laboratory devices as to their susceptibility to non-linear instability is as follows:[74,75,76]

$$\Pi = \frac{\alpha / f}{2R_\infty / \overline{P}} \tag{7}$$

In this expression, α is the linear growth rate of an oscillation, f is the frequency, R_∞ is the limiting amplitude of an oscillation and $\overline{P}$ is the mean pressure.

5. The susceptibility to pulsed instability increases with increasing chamber pressure.[40,45,46,52,60,61] Figure 10 illustrates this. Furthermore, the triggering pulse amplitude, i.e., the pulse amplitude needed to cause instable combustion, decreases as the motor pressure is increased.[45,52,59,68]

6. In general, the lower the motor mean gas velocity, the more likely a motor can be pulsed or triggered into non-linear instability.[15,17,40,45,46,52,77] Lower mean velocities result from higher motor operating pressures and happen later in burn due to a greater cross-sectional area of the chamber.

7. The amount of flow reversal in the forward end of a motor from a pulse can contribute to the triggering behavior of a pulse to cause non-linear instability.[57,61] This is related to (6) above, since more flow reversal can occur when the mean flow velocity is lower.

8. There is direct relationship between DC pressure shifts and limiting amplitude of the oscillations for a motor experiencing pulsed non-linear instability.[40,45,46,52] Figure 14 supports this assumption. It is important to note that the slope of the line in Figure 14 is dependent upon propellant, geometry, chamber pressure and other motor specifics.

9. Oscillatory decay rates from motor pulses are independent of pulse amplitude.[40,45,46,52,59,68,77] This is only true up to the triggering pulse amplitude at which time the motor will be unstable. The growth rate of unstable oscillations will then remain independent of pulse amplitude for pulses greater than the triggering amplitude. High pulse amplitudes can excite instability in an otherwise stable motor.

IV. Commonly Performed Computations

These simple calculations can help determine the character of instability and the effect of this instability on motor performance. Finally, some calculations are performed which seem rather unusual, but are performed often enough to be reported here. Also, a section on the T-Burner and how it works is included.

A. Frequency Analysis

With a very rudimentary knowledge of a motor's interior geometry, various natural acoustic frequencies can be computed. From this information and a frequency analysis of an oscillation, it is usually possible to determine how the motor is oscillating.

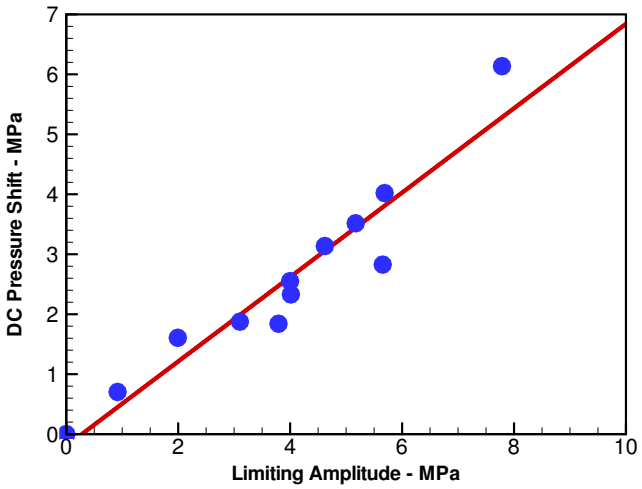

Figure 14. Relationship between DC Pressure Shifts and Limiting Amplitude.

1. Longitudinal Modes: The most common form of instability in motors with composite propellants results in longitudinal acoustic waves traveling from the head end of a solid motor to the aft end and back again, see Figure 1. These oscillations always have pressure anti-nodes at both ends of the motor. For the first acoustic mode, the pressure node, i.e., where no oscillations are occurring, is at the center. The second mode has an additional anti-node at the center and nodes at the 1/4 and 3/4 point along the longitudinal axis of the motor. Location of the pressure nodes and anti-nodes, except the end anti-nodes, will vary somewhat depending upon internal geometry of the motor. The location of acoustic velocity nodes and anti-nodes is the exact opposite of pressure nodes and anti-nodes. To approximate the frequency of longitudinal modes, the following equation may be used:

$$F_n = \frac{na}{2L} \tag{8}$$

Where: n Acoustic mode number, i.e., 1 for first mode, 2 for second mode, *etc*.
a Actual speed of sound in motor cavity, approximate values are 2900 and 3500 ft/sec for metallized and reduced/minimum smoke propellants, respectively
L Chamber length in feet

2. Transverse modes: Transverse acoustic modes include both tangential and radial mode oscillations, see Figure 1. Tangential mode oscillations are most common in double base propellants and hardly ever seen in metallized propellants. Radial modes are very seldom seen in solid rockets and more commonly seen in liquid propulsion rockets engines. Combination modes are also quite rare, but do happen occasionally. Nodes and anti-nodes for tangential modes are not well defined, since these modes can actually rotate with in the motor. Internal geometry such as slots, however, can cause these modes to stay stationary. A frequency spectrum of a transverse mode will show a decrease in frequency as the motor burns, since internal diameters are getting larger. The following equation can be used to approximate transverse modes:

$$F_{\rho,\tau} = \frac{(\alpha_{\rho,\tau})\,a}{2R} \tag{9}$$

Where: a Speed of sound, see Eq. (8)
R Internal radius at time of instability
$\alpha_{\rho,\tau}$ mode coefficient, see Table 1
τ Tangential mode number
ρ Radial mode number

Table 1. Tangential and Radial Mode Coefficients

τ \ ρ	0	1	2	3
0	0	1.220	2.233	3.238
1	0.586	1.697	2.714	3.726
2	0.972	2.135	3.173	4.192
3	1.337	2.551	3.611	4.643

Example: Determine first tangential mode coefficient, $\rho = 0$ and $\tau = 1$, then the coefficient to use is, $\alpha_{0,1}$=0.586.

3. Omega, Non Dimensional Frequency: The non-dimensional frequency, omega-Ω, is often used by theoreticians to understand the nature of the instability.[1,78,79] Many composite propellants whose pressure-coupled response has been evaluated by the T-burner have a response peak with an omega value of between 5 and 30 and often has a value around 10.[57,80] It is the ratio of the acoustic time to the thermal conduction time. It is computed by the following:

$$\Omega = \frac{2\pi f \eta}{\bar{r}^2} \tag{10}$$

Where: f frequency in cycles per second
η thermal diffusivity
$\bar{r}$ burning rate in units of in/sec

In this expression, η/r^2 is the characteristic time of the thermal wave. Some typical values of thermal diffusivity in units of in^2/sec can be found in Table 2.

Table 2. Typical Thermal Diffusivity Values.

Propellant Family	Value
PBAN AP	2.64 x 10-4
Polyurethane-no Al	1.82 x 10-4
Pure AP	3.45 x 10-4
PBAN based with 10% Al	3.25 x 10-4
Aluminized Polyurethane	2.80 x 10-4
Aluminized HTPB or PBAN	1.60 x 10-4

B. Thrust Oscillations Due To Pressure Oscillations

Once a motor does experience pressure oscillations, it is often desirable to know what impact these oscillations will have on thrust of the motor. Many people incorrectly assume that all one needs to do is multiply the nozzle area by the peak-to-peak pressure oscillation. This is incorrect, and will yield much smaller oscillations than actually will occur. It is also incorrect that the severity of the thrust oscillations will be the same as the pressure oscillations, i.e., the magnitude of the oscillation over the mean value. In fact, thrust oscillation severity is almost always worse than that of the pressure oscillations. The following two approximate methods assume longitudinal oscillations. Transverse modes usually cause no thrust oscillations. The first method is a quick and dirty method which is always very conservative. It will yield larger thrust oscillations than actually occur. It provides a good upper limit to thrust oscillations. It is as follows:

$$\Delta F = 2 A_C \Delta P \tag{11}$$

Where: ΔF Thrust oscillations
A_C Chamber cross-sectional area
ΔP Peak to peak pressure oscillations

The factor of "2" arises from the fact that pressure oscillations act not only on the nozzle but on the aft and forward end of the motor as well. Since pressure anti-nodes at the motor ends are 180^0 apart, a positive delta pressure acts on one end and a negative delta pressure acts on the other end. A more exact method is as follows:

$$\Delta F = \left[F + P_A A_E - (\bar{P}_N + \bar{P}_H) A_C \right] \frac{\Delta P}{\bar{P}_N} \tag{12}$$

Where: ΔF Thrust oscillations
ΔP Peak-to-peak pressure oscillations
F Mean thrust at ambient pressure
A_E Nozzle exit area
A_C Chamber cross-sectional area at time of oscillation
P_A Ambient pressure
$\bar{P}_N$ Nozzle end pressure
$\bar{P}_H$ Head end pressure

Equation (12) includes the following assumptions: frictionless flow, constant cross sectional area in motor, oscillations at head and aft end equal and 180 phase between head and aft ends. One should notice that as a motor burns, thrust oscillations become worse for the same pressure oscillations because the chamber cross sectional area is increasing. An alternate form of this equation is sometimes written as thrust change per psi of oscillation:

$$\frac{\Delta F}{\Delta P} = \frac{F + P_A A_E - (\bar{P}_N + \bar{P}_H) A_C}{\bar{P}_N} \tag{13}$$

An example of how to use these thrust oscillation equations is as follows:

Assume: F = 10000 lbs
A_E = 20 in^2
A_C = 80 in^2
P_A = 10 psi
$\bar{P}_N$ = 990 psi
$\bar{P}_H$ = 1010 psi

$$\frac{\Delta F}{\Delta P} = \frac{10000\,lbs + (10\,psi)(20\,in^2) - (990\,psi + 1010\,psi)80\,in^2}{990\,psi}$$

$$= 151\frac{lbs}{psi}$$

This means that for every single psi of pressure oscillation the motor will produce 150 pounds of thrust oscillation. The short method would say 160 pounds per oscillatory psi.

C. Combustion Gas Velocity Calculation

The combustion gas velocity is the velocity at which the gaseous solid propellant combustion products move perpendicularly away from the surface. The computation of this parameter is important to estimate the velocity of burning metal particles leaving the surface to determine if distributed combustion is taking place. To approximate gas velocity from a burning propellant, first an assumption is made that the gases follow the ideal gas law and the density and the velocity of the gas are given by:

$$\rho = \frac{PM}{RT} \qquad\qquad v_{gas} = r_{propellant}\left(\frac{\rho_{solid}}{\rho_{solid}}\right) \tag{14,15}$$

In general, the approximate gas velocity can be given by the following table. The further you are from the base pressure and burning rate given in Table 3, the more the error will be in these approximations. The injection Mach number is typically around 0.0029.

Table 3. Gas Ejection Velocity Approximations

Gas Velocity	Propellant type and burning rate condition
v = 23858 (r/p)	Metallized propellant at 1000 psi and 0.5 in/sec, v = 11.93 ft/sec
v = 20075 (r/p)	Reduced smoke propellant at 1000 psi and 0.5 in/sec, v = 10.04 ft/sec
v = 24550 (r/p)	High burning rate metallized propellant at 3000 psi and 5.0 in/sec, v = 40.92 ft/sec

D. T-Burner Theory and Pressure-Coupled Response Determination

The standard way to measure the combustion response is by the T-burner.[7] The T-Burner has been around in one form or another since 1958 and is shown in Figure 15. Two disks of propellant of equal thickness are placed on each end of a 1.5-inch diameter pipe combustor and they are ignited simultaneously. Ideally, they will also burn out simultaneously. The geometry of the T-Burner was designed to provide an environment which is ideally suited to study the effect of acoustic pressure oscillations on solid rocket propellant. Assuming a 1st longitudinal mode, like the one shown in Figure 1 is present in the burner, the maximum driving in the T-Burner is at the ends where the pressure oscillations are a maximum and all the propellant is located. The acoustic velocity, cross flow velocity and mean flow are all zero at the ends as to isolate the pressure-coupled response. The test frequency depends on the burner length and the combustion gas temperature. Data are obtained by pulsing the burner during the propellant burn and after burn out. The pressure amplitude rate of change of the oscillations is measured by a piezoelectric quartz pressure transducer. To determine when burnout occurs, phototransistors are located at each end to measure the light output at burnout. For some propellants, pulsing is not required and the T-burner acoustic oscillations grow spontaneously. In either case, the difference between the alpha during sample burn, α_1, and the decay alpha after burnout, α_2, is known as the combustion alpha, α_c.

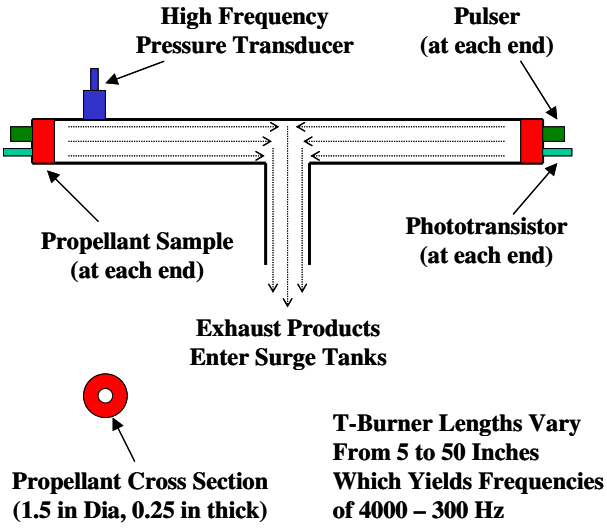

Figure 15. T-Burner Diagram

$$\alpha_C = \alpha_1 - \alpha_D \quad \text{while} \quad \alpha_D = \alpha_2(f_1) \qquad (16, 17)$$

Where: α_1 pressure decay rate constant during burn
$\alpha_2(f_1)$ pressure decay constant after burning with correction to frequency of α_1

From the computed, α_C, burner length and propellant properties, the combustion response is computed from:

$$R_{pc} = \frac{\alpha_C \overline{P}}{4 f a \rho_p \bar{r}_b (S_B/S_C)} \left(\frac{a_m}{a}\right) \qquad (18)$$

Where: $\overline{P}$ mean pressure
f frequency
ρ_p propellant density
$\bar{r}_b$ measured burning rate
S_B/S_C propellant burning surface area to channel area ratio
a theoretical gas speed of sound
a_m measured speed of sound, $a_m = 2fL$, L = burner length

V. Motor Instrumentation

This section is just to remind motor designers and test personnel that combustion instability in rocket motors can only be examined if the test motor is instrumented correctly. It is strongly recommended that all development motors be instrumented to observe combustion instability. Even if no instability is measured, test records provide a starting point if, at some point in the motor's lifetime, a problem does occur. The following lists important points for good motor instrumentation for examining combustion instability behavior. Reference 40 contains an excellent review of motor instrumentation as well as data reduction methods.

1. Pressure data is always preferred over strain gage or accelerometer data.

2. Piezoelectric high frequency quartz crystal pressure gages should be used whenever possible. The only exception to this is for very large motors, like the Space Shuttle SRMs where very high frequency response is not needed. Figure 16 depicts a suggested motor instrumentation data path for high frequency pressure measurement.

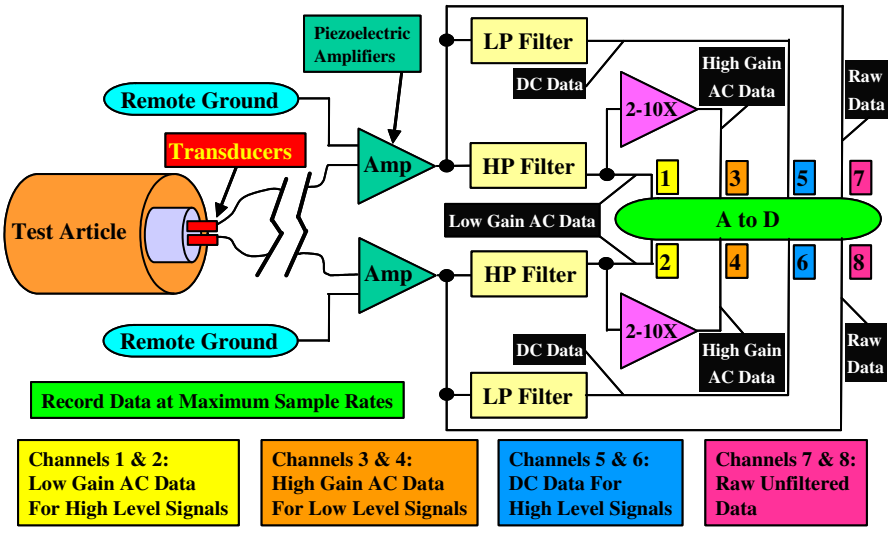

Figure 16. Motor Pressure Instrumentation Data Path

3. A conventional strain-gage low frequency pressure transducer should also be used to monitor steady-state chamber pressure and accurately measure any possible DC pressure shifts.

4. The best place to measure longitudinal modes is at either end of the motor where the acoustic pressure anti-nodes are located.

5. The best place to measure transverse modes is one gage mounted at 0^0 and one at 120^0 around the motor case near where the oscillation is occurring. This is often impossible; however, so gages mounted at the end of the motor, near the outside radius at 0^0 and 120^0 may be used. Often, the end-mounted gages will work, but measured amplitudes may be wrong.

6. Whenever possible, use redundant gages. Full-scale motor firings are too expensive not to take the extra insurance.

7. Pressure gages should be as close to the motor chamber as possible, i.e., very close-coupled to the chamber pressure. High frequency gages mounted on extension tubes can loose their frequency response and the use of extension tubes can add acoustic modes that are not part of or even related to actual chamber oscillations. The resonant frequency of a cavity installation is inversely proportional to the passage length and can be determined from the following equation.[81]

$$f = \frac{a}{4\,(L + 0.85D)} \tag{19}$$

In this equation, a is the speed of sound in the cavity, L is the passage length and D is the passage diameter. For short cavities that are on the order of the transducer diameter, this resonant frequency is very high usually does not interfere with measurements of the acoustic pressure oscillations taking place in the motor chamber. As the cavity length increases, sharp fronted pressure waves may excite the passage to resonance, an organ pipe effect, and mask the true behavior pressure oscillations.

VI. Conclusions

This report has brought together many facets of combustion instability: theoretical issues dealing with driving and damping mechanisms; motor stability prediction and various theoretical observations, and empirical observations about oxidizer particle size, propellant burning rate, mean flow, particle, chemistry and non-linear effects were all addressed. Also presented were various commonly performed computations, including how to estimate a motor's longitudinal and transverse acoustic modes, thrust oscillation prediction, gas velocity calculations and a brief description on how a T-burner works. In addition, a short section dealing with motor instrumentation to monitor combustion instability was discussed. It is hoped that this paper will aid motor designers and motor firing data analysis to better understand what causes and, most importantly, how to prevent combustion instability.

VII. Acknowledgements

The author wishes to thank all of the people who gave advice and suggested references for this paper. Special thanks go the Merrill Beckstead, Woodward Waesche, Jay Levine, Norman Cohen, Ed Price and Gary Flandro. Also I wish to thank James Crump and H.B. Mathes who provided guidance during my first ten years at China Lake.

VIII. References

[1] L. De Luca, E.W. Price and M. Summerfield, "Nonsteady Burning and Combustion Stability of Solid Propellants," *Progress in Astronautic and Aeronautics, Volume 143*, Published by the AIAA, Washington, DC, 1992.

[2] F.S. Blomshield, "Historical Perspective of Combustion Instability in Motors: Case Studies," 37th AIAA Propulsion Conference, Paper No. 2001-3875, Salt Lake City, Utah, July 2001.

[3] R.S. Brown, "Combustion Stability Of Interceptor Rocket Motors: A Practical Approach To Managing Instability Problems," CPTR 95-57, Chemical Propulsion Information Agency, June 1995.

[4] F.E.C. Culick, "Unsteady Motions in Combustion Chambers for Propulsion Systems," NATO Research and Technology Organization, RTO-AG-AVT-039, http://www.rta.nato.int, September 2006.

[5] F.E.C. Culick, "Combustion Instability in Solid Rocket Motors, Volume II: A Guide for Motor Designers," CPIA Publication 290, January 1981.

[6] F.S. Blomshield, R.A. Stalnaker and M.W. Beckstead, “Combustion Instability Additive Investigation,” AIAA Joint Propulsion Meeting, Paper No. 99-2226, Los Angeles, CA, June 1999.
[7] F.E.C. Culick, "T-burner Manual," CPIA Publication No. 191, November 1969.
[8] M.W. Beckstead, K.V. Meredith and F.S. Blomshield, “Examples Of Unsteady Combustion In Non-Metallized Propellants,” Presented at the 36th JANNAF Combustion Meeting, CPIA Pub. 697, pp. 59-75, Cocoa Beach, Florida, October 1999.
[9] R.S. Brown, J.E. Erickson and W.R. Babcock, "Combustion Response Function Measurements by the Rotating Valve Method," *AIAA Journal*, Vol. 12, pp. 1502-1510, November 1974.
[10] J.R. Wilson and M.M. MICCI, “Direct Measurement of High Frequency, Solid Propellant, Pressure-Coupled Admittances,” *Journal of Propulsion and Power*, Vol. 3, No. 4, 1987, pp. 296-302.
[11] A.D. Johnston, T.W. Park, G.L. Vogt and L.D. Strand, "Microwave Doppler Shift Measurement of Solid Propellant Combustion Response Function," AFAL TR-87-082, September 1987.
[12] S.F. Son and M.Q. Brewster, “Linear Burning Rate Dynamics of Solids Subjected to Pressure or External Radiant Heat Flux Oscillations**,”** Journal of Propulsion and Power, Vol. 9, No. 2, 1993, pp. 222-232.
[13] J.C. Finlinson, D. Hanson-Parr, S.F. SON, and M.Q. Brewster, “Measurement of Propellant Combustion Response to Sinusoidal Radiant Heat Flux,” 29th AIAA Aerospace Sciences Meeting, Paper No. 1991-204, Reno, NV, January 1991.
[14] F.E.C. Culick, "An Introduction to Velocity Coupling in Solid Propellant Rockets," NWC-TP-6464, Naval Air Warfare Center, China Lake, February 1983.
[15] J.D. Baum , J.N. Levine and R.L. Lovine, “Pulsed Instabilities in Rocket Motors: A Comparison between Predictions and Experiments, “*Journal of Propulsion and Power*, Vol. 4, No. 4, 1988, pp. 308-316.
[16] V. Yang and J.I.S. Tseng, "Numerical Simulation of Velocity-Coupled Combustion Response of Solid Rocket Propellants," PL-TR-91-3043, February 1992.
[17] R.S. Brown, A.M. Blackner, P.G. Willoughby and R. Dunlap, "Coupling Between Velocity Oscillations and Solid Propellant Combustion," Final Technical Report, Director of Aerospace Sciences, AFOSR, August 1986.
[18] F.S. Blomshield, K.J. Kraeutle, R.A. Stalnaker, M.W. Beckstead and B. Stokes, "Aluminum Combustion Effects on Combustion Instability of High Burn Rate Propellants," 28th JANNAF Combustion Meeting, CPIA Publication 573, Vol. III, pp. 419-438, October 1991.
[19] M.W. Beckstead and K.P. Brooks, "A Model for Distributed Combustion in Solid Propellants," 27th JANNAF Combustion Meeting, CPIA Publication 557, Vol. II, pp. 237-258, November 1990.
[20] F.E.C. Culick, "Stability of Longitudinal Oscillations with Pressure and Velocity Coupling in Solid Propellant Rocket," *Combustion Science and Technology*, Vol. 2, pp. 179-201, 1970.
[21] F.E.C. Culick, "The Stability of One-Dimensional Motions in A Rocket Motor," *Combustion Science and Technology,* Vol. 7, pp. 165-175, 1973.
[22] B.T. Zinn, W.A. Bell, B.R. Daniel and A.J. Smith, "Experimental Determination of Three-Dimensional Liquid Rocket Nozzle Admittances," *AIAA Journal*, Vol. 11, No. 3, pp. 267-272, 1973.
[23] F.E.C. Culick, "Stability of Three-Dimensional Motions in a Combustion Chamber," *Combustion Science and Technology*, Vol. 10, pp. 109-124, 1975.
[24] S. Temkin and R.A. Dobbins, "Attenuation and dispersion of Sound by Particulate Relaxation Processes," *Journal or Acoustic Society of America*, Vol. 40, No. 2, pp. 317-324, 1966.
[25] S. Temkin and R.A. Dobbins, "Measurements of Attenuation and dispersion of Sound by an Aerosol," *Journal or Acoustic Society of America,* Vol. 40, No. 5, pp. 1016-1024, 1966.
[26] G.L. Dehority and K.J. Kraeutle, "Procedure for the Calculation of Particulate Damping of Acoustic Oscillations," NWC TM 2889, Naval Air Warfare Center, September 1976.
[27] K.J. Kraeutle, R.L. Derr, H.B. Mathes and G.L. Dehority, "Combustion Instability Studies Using Metallized Solid Propellants: Additional Experimental Evidence for the Validity of Particle Damping Theory," 12th JANNAF Combustion Meeting, CPIA Publication No. 273, Vol. II, pp. 155-165, December 1975.
[28] F.E.C. Culick, "Remarks on Entropy Production in the One-Dimensional Approximation to Unsteady Flow in Combustion Chambers," *Combustion Science and Technology*, vol. 15, pp. 93-97, 1977.
[29] A.S. Hersch and J. Tso, "Flow Turning Losses in Solid Rocket Motors," AFAL-TR-87-095, March 1988.
[30] G.A. Flandro, "Solid Propellant Acoustic Admittance Corrections," *Journal of Sound and Vibration*, Vol. 36, pp. 297-312, 1974.
[31] G.A. Flandro, “Energy Balance Analysis of Nonlinear Combustion Instability,” *Journal of Propulsion and Power*, Vol. 1, No. 3, 1985, pp. 210-221.
[32] F. Vuillot and G. Avalon, “Acoustic Boundary Layer in Large Solid Propellant Rocket Motors Using Navier-Stokes Equations,” *Journal of Propulsion and Power*, Vol. 7, No. 2, 1991, pp. 231-239.
[33] G.A. Flandro, “Effects of Vorticity on Rocket Combustion Stability,” *Journal of Propulsion and Power*, Vol. 11, No. 4, 1995, pp. 607-625.
[34] R.S. Brown, R. Dunlap, S.W. Young, G.A. Flandro, L.K. Isaacson, R.A. Beddini and R.E.C. Culick, "Vortex Shedding Studies," AFRPL-TR-80-13, April 1980.

[35] M.C. Dawson, W.C. Andrepont, D.L. Luther and G.A. Flandro, "Elimination of Flow Induced Instabilities in solid Rocket Motors by Aerodynamic Contouring of Internal Grain Geometries - A Final Report," 18th JANNAF Combustion Meeting, CPIA Publication No. 347, Vol. I, pp. 9-21, October 1981.
[36] R. Dunlap, J.S. Sabnis, R.A. Beddini, G.A. Flandro, R.S. Brown, H.J. Gibeling, A.M. Blackner, R.C. Waugh and H. McDonald, "Internal Flow Field Investigation," AFRPL-TR-85-079, November 1985.
[37] R.S. Brown, R. Dunlap, S.W. Young, and R.C. Waugh, "Vortex Shedding as a Source of Acoustic Energy in Segmented Solid Rockets," *Journal of Spacecraft and Rockets*, Vol. 18, 1981, pp. 312–319.
[38] F.S. Blomshield and H.B. Mathes, "Pressure Oscillations in Post-Challenger Space Shuttle Redesigned Solid Rocket Motors," *AIAA Journal of Propulsion and Power*, Vol. 9, No. 2. pp. 217-221, March-April 1993.
[39] F.S. Blomshield and C.J. Bicker, "Pressure Oscillations in Shuttle Solid Rocket Motors," 1997 AIAA Joint Propulsion Meeting, Paper No. 97-3252, Seattle, Washington, July 1997.
[40] F.S. Blomshield, J.E. Crump, H.B. Mathes and M.W. Beckstead, "Stability Testing and Pulsing of Full Scale Tactical Motors," NAWCWPNS-TP-8060, Naval Air Warfare Center, Weapons Division, China Lake, CA, July 1992.
[41] F.S. Blomshield, J.E. Crump, H.B. Mathes, R.A. Stalnaker and M.W. Beckstead, "Stability Testing of Full-Scale Tactical Motors," *AIAA Journal of Propulsion and Power*, Vol. 13. No. 3, pp. 349-355, May-June 1997.
[42] F.S. Blomshield, C.J. Bicker and Richard A. Stalnaker, "High Pressure Pulsed Motor Firing Combustion Instability Investigations," 1997 AIAA Joint Propulsion Meeting, Paper No. 97-3253, Seattle, Washington, July 1997.
[43] F.S. Blomshield and R.A. Stalnaker, "Pulsed Motor Firings: Pulse Amplitude, Formulation and Enhanced Instrumentation," 34th AIAA Joint Propulsion Meeting, Paper No. 98-3557, Cleveland, Ohio, July 1998.
[44] F.S. Blomshield, C.J. Bicker and Richard A. Stalnaker, "High Pressure Pulsed Motor Firing Combustion Instability Investigations," 1997 AIAA Joint Propulsion Meeting, Paper No. 97-3253, Seattle, Washington, July 1997.
[45] F.S. Blomshield, "Pulsed Motor Firings," NAWCWD TP 8444, March 2000.
[46] F.S. Blomshield, "Pulsed Motor Firings," *Chapter on Solid Propellant Chemistry, Combustion, and Motor Interior Ballistics*, edited by V. Yang, T. B. Brill, and W. Z. Ren, Vol. 185, *AIAA Progress in Astronautics and Aeronautics*, Reston, VA, July 2000.
[47] G.R. Nickerson, F.E.C. Culick and A.L. Dang, "The Solid Propellant Rocket Motor Performance Computer Program (SPP) Version 6.0," AFAL-TR-87-078, December 1987.
[48] French, J.C., Coats, D.E., "Automated 3-D Solid Rocket Combustion Stability Analysis", 35th AIAA Joint Propulsion Conference, Paper No. 1999-2797, Los Angeles, CA, 1999.
[49] French, J.C. and Dunn, S.S., "New Capabilities in Solid Rocket Motor Grain Design Modeling (SPP'02)", 38th JANNAF Combustion Subcommittee, Destin, FL, 2002.
[50] Coats, D.E., French, J.C., Dunn, S.S., Berker, D.R., "Improvements to the Solid Performance Program (SPP)", 39th AIAA Joint Propulsion Conference, 2003-4668, Huntsville, AL, July 2003.
[51] French, J.C., "Non-Linear Combustion Stability Prediction of SRMs using SPP / SSP", 39th AIAA Joint Propulsion Conference, Paper No. 2003-4668, Huntsville, AL, July 2003.
[52] F.S. Blomshield, H.B. Mathes, J.E. Crump, C.A. Beiter and M.W. Beckstead, "Nonlinear Stability Testing of Full-Scale Tactical Motors," *AIAA Journal of Propulsion and Power*, Vol. 13. No. 3, pp. 356-366, May-June 1997.
[53] R.L. Lovine, "Non-Linear Stability for Tactical Motors, Volume V - Propellant Screening Methodology, Parts 1 and 2," AFRPL-TR-85-017, February 1985.
[54] J.E. Crump, "Combustion Instability In Minimum Smoke Propellants, Part 1. Experimental Techniques and Results," NWC-TP-5936, Part 1, Naval Air Warfare Center, China Lake, November 1977.
[55] T.P. Rudy, H.H. Weyland, E.J. Shanabrook, R.S. Brown, L.S. Bain and G.A. Flandro, "High Pressure Characterization," AFAL-TR-88-053, July 1988.
[56] W.R. Waesche, Personal Communications, Gainesville, Virginia, 1992.
[57] M.W. Beckstead, Personal Communications, Brigham Young University, Provo, Utah, 2006.
[58] N.S. Cohen, "Modeling Plateau Ballistics in Energetic Binder Propellants," 28th JANNAF Combustion Meeting, CPIA Publication 573, Vol. III, pp. 493-504, October 1991.
[59] W.G. Brownlee, "Non-Linear Axial Combustion Instability in solid Propellant Motors," *AIAA Journal*, Vol. 2, pp. 275-284, February, 1964.
[60] R.L. Lovine and P.L. Micheli, "Non-Linear Stability for Tactical Motors: Volume I - Program Summary," AFRPL-TR-85-017, October 1985.
[61] P.L. Micheli, "Non-Linear Stability for Tactical Motors: Volume II - Mechanism Study," AFRPL-TR-85-017, February 1986.
[62] F.S. Blomshield, "Nitramine Composite Solid Propellant Modeling," NWC-TP-6992, Naval Air Warfare Center, China Lake, July 1989.
[63] H.B. Mathes, "Assessment of Chamber Pressure Oscillations in the Shuttle solid Rocket Booster Motor," AIAA Propulsion Conference, Paper No. 80-1091, 1980.
[64] F.S. Blomshield and H.B. Mathes, "Pressure Oscillations in Post-Challenger Space Shuttle Redesigned Solid Rocket Motors (RSRM)," 29th AIAA Aerospace Sciences Meeting, Paper No. 91-0203, Reno, Nevada, January 1991.

[65] B.A. Janardan and B.T. Zinn, "Effect of Nozzle Submergence upon Stability of Solid Rockets," *AIAA Journal*, Vol. 14, No. 1, January 1976.
[66] French, J.C., "Tangential Mode Instability of SRMs with Even and Odd Numbers of Slots", 38th AIAA Joint Propulsion Conference, paper 2002-3612, July 2002.
[67] M.W. Beckstead and E.W. Price, "Non-Acoustic Combustor Instability," *AIAA Journal* Vol. 5, No. 11, pp. 1989-1996, 1967.
[68] F.S. Blomshield and M.W. Beckstead, "Non-Linear Characteristics of Solid Propellant Combustion Instability," 29th JANNAF Combustion Meeting, CPIA Pub. 593, Vol. 4, pp. 197-207, NASA Langley, Virginia, October 1992.
[69] M.W. Beckstead, "Potential Combustion and Combustion Instability Characteristics of CL-20 Propellants," 28th JANNAF Combustion Meeting, CPIA Publication 573, Vol. III, pp. 369-377, October 1991.
[70] T. Parr and D. Hanson-Parr, "Propellant Diffusion Flame Structure," 28th JANNAF Combustion Meeting, CPIA Publication 573, Vol. III, pp. 359-368, October 1991.
[71] J.D. Baum, J.N. Levine and R.L. Lovine, "Pulse Triggered Instability in Solid Rocket Motors," *AIAA Journal*, vol. 22, No. 10, pp. 1413-1419, October 1984.
[72] J.D. Baum and J.N. Levine, "Modeling of Non-Linear Combustion Instability in Solid Propellant Rocket Motors," AFRPL-TR-83-058, February 1984.
[73] P.L. Micheli and G.A. Flandro, "Non-Linear Stability for Tactical Motors, Volume III - Analysis of Non-Linear Solid Propellant Combustion Instability," AFRPL-TR-85-017, February 1986.
[74] M.W. Beckstead and R.C. Jensen, "Non-Linear Interpretation of Linear T-Burner Data," 9th JANNAF Combustion Meeting, CPIA Publication 231, Vol. I, pp. 239-247, September 1972.
[75] R.C. Jensen and M.W. Beckstead, "Non-Linear Analysis of Combustion Instability Data," 10th JANNAF Combustion Meeting, CPIA Publication 243, Vol. II, pp. 163-177, December 1973.
[76] M.W. Beckstead, "Non-Linear Mechanisms of Solid Propellant Combustion Instability," 24th JANNAF Combustion Meeting, CPIA Publication 476, Vol. I, pp. 27-40, October 1987.
[77] R.L. Lovine, "Non-Linear Stability for Tactical Motors: Volume IV - Pulsing Considerations, Parts 1 and 2," AFRPL-TR-84-017, August 1985.
[78] M.R. Denison and E. Baum, "A simplified Model of Unstable Burning in Solid Propellants," *American Rocket Society Journa*l, pp. 1112-1122, August 1961.
[79] F.E.C. Culick, "A Review of Calculations for Unsteady Burning of a Solid Propellant," *AIAA Journal*, Vol. 6, Number 12, pp. 2241-2255, December 1968.
[80] N.S. Cohen and B.B. Stokes, "High Frequency Combustion Instability of Reduced-Smoke Propellant, A Case Study," 28th JANNAF Combustion Meeting, CPIA Publication 573, Vol. III, pp. 451-462, October 1991.
[81] Kistler Instrument Corporation, “Operating Instructions: Universal Pressure Transducers, Types 211B(X), 601B(X) and 601B(X),” Amherst, NY, 2006.